JOURNAL OF CATALYSIS 139, 435–443 (1993)

Catalytic Properties of ZSM-5 Zeolites in N_2O Decomposition: The Role of Iron

VLADIMIR I. SOBOLEV, GENNADY I. PANOV, ALEKSANDR S. KHARITONOV, VYACHESLAV N. ROMANNIKOV, ALEKSANDR M. VOLODIN, AND KAZIMIRA G. IONE

Institute of Catalysis, Novosibirsk 630090, Russia

Received July 1, 1991; revised April 27, 1992

Ferrisilicate analogues of ZSM-5 zeolite have been found to be efficient catalysts for direct oxidation of benzene to phenol using dinitrogen monoxide as an oxidant. The reaction of N_2O decomposition over these catalysts has now been studied. Specific active sites (referred to as α-sites) consisting of Fe atoms have been shown to be responsible for catalytic properties of ferrisilicates. Decomposition of N_2O on α-sites generates a reactive form of surface oxygen which cannot be produced by O_2 adsorption. The concentration of α-sites and the rate of N_2O decomposition as functions of iron content over the wide range of its concentrations (from 0.003 to 4.8 wt% Fe_2O_3) have been studied. When comparing these data with the previous results for ZSM-5 zeolites of ferrialuminosilicate composition, the properties of α-sites have been shown to be identical in both systems. The superior activity of Fe–Al–Si samples to that of Fe–Si samples is accounted for by a higher concentration of α-sites in the former at the same iron content, caused by the favourable influence of Al on Fe distribution throughout the zeolite matrix.

INTRODUCTION

Since the 1950's the decomposition of dinitrogen monoxide has begun to be extensively used as a model reaction when studying mechanisms of catalysis and revealing relations between physicochemical and catalytic properties of solids (*1*). In recent years this reaction has evoked renewed interest because N_2O has become employed as an oxidant especially in studying the mechanism of oxidative conversion of methane and other low paraffins. Substitution of molecular dioxygen by dinitrogen monoxide occasionally results in a significant increase in reaction selectivity (*2–7*). N_2O and O_2 as oxygen donors for oxidative coupling of methane has been compared by Hutchings *et al.* (8).

The efficiency of dinitrogen monoxide as an oxidant has been highlighted in the reaction of direct oxidation of benzene to phenol—a delicate and difficult reaction which long failed to be performed with appropriate selectivity if dioxygen was used. Iwamoto *et al.* were the first who achieved the reaction over supported oxides of vanadium, molybdenum, or tungsten (*9*). Oxidation of benzene by N_2O over these catalysts occurred at 500–600°C with selectivity as high as 71%. This promising result stimulated a further search for more effective catalysts. In 1988 three teams of researchers (*10–12*) discovered independently a new catalytic system of far superior efficiency—ZSM-5 zeolites. Oxidation of benzene takes place over these catalysts at 300–400°C and, what is more, with a very high selectivity for phenol (up to 100%).

It is worth mentioning that the reaction proceeds only in the presence of N_2O. There is no phenol formation if N_2O is substituted by O_2. The reaction of oxidative hydroxylation using dinitrogen monoxide has lately been applied to other aromatic compounds (*13*, *14*).

These results call a considerable interest in N_2O decomposition as the reaction stage supplying surface whose properties seem to be of crucial importance. The relation be-

0021-9517/93 $5.00

tween the presence of iron and the reactions of both benzene oxidation and N_2O decomposition was shown in studying ZSM-5 zeolites of aluminosilicate composition ($Al_2O_3/SiO_2 = 100$) (*15–17*). The introduction of Fe into the Al–Si zeolite matrix leads to the formation of specific sites (hereafter referred to as α-sites) where the decomposition of N_2O is accompanied by generation of a reactive form of surface oxygen (α-form) which cannot be produced by O_2 adsorption. This form is a very probable reason for the unique catalytic performance of FeZSM-5 zeolites in benzene to phenol oxidation. When introduced in ZSM-5, other metals than iron (Ti, Cr, Mn, Ni, Cu, Zn, Pd, Pt) have no sign of catalytic activity in this reaction.

The oxidation of benzene by dinitrogen monoxide was recently investigated over another series of Fe-containing zeolites: ferrisilicate analogues of ZSM-5 (*18*). In spite of some important differences the efficiency of Fe–Si samples is as high as that of the Fe–Al–Si samples studied before. It would therefore be interesting now to carry out a parallel investigation of N_2O decomposition over this system in particular in order to elucidate (i) if ferrisilicate samples are active in this reaction too; (ii) to what extent and in which way this activity is connected with the presence of iron; and (iii) if the formation of α-oxygen occurs on Fe–Si samples upon N_2O decomposition. Along with previous data for the Fe–Al–Si system it would provide more complete information about catalytic properties of Fe introduced and about the influence of the chemical composition of zeolite matrix as well.

EXPERIMENTAL

Catalysts. In this work the same samples of ferrisilicates were used as were studied in the reaction of benzene oxidation (*18*). Zeolites were synthesized by the hydrothermal method according to (*19*) with iron introduced into the starting gel as $Fe_2(SO_4)_3$. The samples were acidified by treatment with ammonia buffer solution followed by calcination in air at 600°C. The concentration of iron ranged from 0.003 to 4.8 wt% Fe_2O_3 (Table 1). The formula Fe-x is used to designate the samples, where x denotes the weight percentage of Fe_2O_3.

In addition to iron, Al and Na content in the samples was found by atomic adsorption, being 0.01–0.03 wt% Al_2O_3 for the former and 0.01–0.06 wt% Na_2O for the latter. The degree of zeolite crystallinity was determined by X-ray analysis to be above 95% for all the samples.

The samples of bulk and supported iron oxides were also studied to compare them with zeolites (Table 1). The sample Fe_2O_3/SiO_2-3.0 was SiO_2 (aerosil) on which 3.0 wt% of Fe_2O_3 was loaded by impregnation with aqueous solution of $Fe(NO_3)_3$. After being dried at 120°C the sample was calcinated in air at 550°C for 2 h. Surface area measured by low temperature adsorption of argon was 200 m^2/g.

The sample of α-Fe_2O_3 was a commercial specimen of "high purity grade" with surface area of 10 m^2/g.

Apparatus. Experimental procedure. The experiments, such as N_2O decomposition, isotope oxygen exchange, and oxidation of CO and CH_4, were carried out in a vacuum static apparatus equipped with an on-line mass spectrometer for gas-phase analysis. In the apparatus vacuum was provided up to 1×10^{-7} Torr. A working section was isolated from vacuum pumps by a metal trap which was cooled with liquid dinitrogen. There were facilities for temperature-programmed heating of a sample. A catalyst sample (0.3–1.0 g, fraction 0.25–0.5 mm) was placed in a microreactor which could be easily isolated from the rest of the system. A number of advantages in making adsorption and kinetic measurements were provided by the reactor volume (ca. 5 cm^3) being an insignificant part of the total reaction volume (620 cm^3) (*20*).

Before the start of the experiments, samples were subjected to a standard pretreatment consisting of alternate oxidative (1 Torr of O_2) and vacuum treatments at 550°C.

TABLE 1

Catalytic Properties of Iron Containing Samples in the Reaction of N_2O Decomposition

Sample	Iron content		Concentration of active α-sites, $C_{\alpha-s}$ (α-site · g^{-1})	Reaction rate (400°C, 0.4 Torr)			E_{act} (kcal · mol^{-1})
	$C_{Fe_2O_3}$ (wt% Fe_2O_3)	C_{Fe}[a] (Fe · g^{-1})		W_g (molecule · $g^{-1} \cdot s^{-1}$)	W_{Fe}[b] (molecule $Fe^{-1} \cdot s^{-1}$)	TOF[c] (molecule $s^{-1} \cdot s^{-1}$)	
Fe-0.003	0.003	$2.2 \cdot 10^{17}$	not detected ($<1 \cdot 10^{16}$)	$2.7 \cdot 10^{13}$	$1.2 \cdot 10^{-4}$	—	—
Fe-0.05	0.05	$3.8 \cdot 10^{18}$	not detected	$3.2 \cdot 10^{13}$	$6.2 \cdot 10^{-6}$	—	—
Fe-0.13	0.15	$1.0 \cdot 10^{19}$	$\sim 1 \cdot 10^{16}$	$1.4 \cdot 10^{14}$	$7.6 \cdot 10^{-6}$	$\sim 1.4 \cdot 10^{-2}$	27
Fe-0.33	0.33	$2.5 \cdot 10^{19}$	$8.5 \cdot 10^{16}$	$1.1 \cdot 10^{15}$	$4.4 \cdot 10^{-5}$	$1.3 \cdot 10^{-2}$	26 ± 1
Fe-1.3	1.3	$1.0 \cdot 10^{20}$	$1.2 \cdot 10^{18}$	$6.5 \cdot 10^{16}$	$6.5 \cdot 10^{-4}$	$5.4 \cdot 10^{-2}$	31 ± 1
Fe-2.1	2.1	$1.6 \cdot 10^{20}$	$3.1 \cdot 10^{18}$	$1.5 \cdot 10^{17}$	$9.5 \cdot 10^{-4}$	$4.8 \cdot 10^{-2}$	30 ± 3
Fe-2.2	2.2	$1.7 \cdot 10^{20}$	$3.5 \cdot 10^{18}$	$1.0 \cdot 10^{17}$	$6.0 \cdot 10^{-4}$	$2.9 \cdot 10^{-2}$	29 ± 5
Fe-4.0	4.0	$3.0 \cdot 10^{20}$	$5.8 \cdot 10^{18}$	$8.2 \cdot 10^{16}$	$2.7 \cdot 10^{-4}$	$1.4 \cdot 10^{-2}$	31 ± 5
Fe-4.8	4.8	$3.6 \cdot 10^{20}$	$8.3 \cdot 10^{18}$	$1.6 \cdot 10^{17}$	$4.4 \cdot 10^{-4}$	$1.9 \cdot 10^{-2}$	31 ± 4
α-Fe_2O_3	100	$1.0 \cdot 10^{20}$	not detected	$4.0 \cdot 10^{14}$	$4.0 \cdot 10^{-6}$	—	33 ± 1.5
Fe_2O_3/SiO_2-3.0	3.0	$2.2 \cdot 10^{20}$	not detected	$2.4 \cdot 10^{14}$	$1.0 \cdot 10^{-6}$	—	32 ± 3

[a] For Fe_2O_3 C_{Fe} referred to the number of surface Fe atoms ($1 \cdot 10^{19}$ Fe · m^{-1}).

[b] For Fe_2O_3 W_{Fe} referred to the number of the surface Fe atoms, for other samples to the total number of Fe atoms.

[c] Turnover frequency as molecules per α-active site per second.

Dinitrogen monoxide of medically pure grade was used. In experiments on isotopic O_2 exchange both "heavy" dioxygen with 85% of isotope ^{18}O and a mixture of "heavy" and natural O_2 (1 : 1) were used. More procedural details are given in (*15*, *16*).

RESULTS

It is characteristic of ZSM-5 zeolites of Fe–Al–Si composition that there are two different regions of the reaction of N_2O decomposition (*15*). Within the low temperature region (below 300°C) the reaction is accompanied by binding of oxygen atoms to active α-sites and comes to an end as the sites are completely loaded:

$$N_2O + (\ \ ) \rightarrow (O) + N_2. \qquad (1)$$

Over the high temperature region (above 300°C) where the desorption of α-oxygen form (O) takes place the reaction proceeds as a "normal" catalytic process followed by evolution of stoichiometric amounts of N_2 and O_2 into a gas phase:

$$\begin{array}{rl} N_2O + (\ \ ) \rightarrow (O) + N_2 & 2 \\ 2(O) \rightarrow O_2 + 2(\ \ ) & 1 \\ \hline 2N_2O \rightarrow 2N_2 + O_2. & (2) \end{array}$$

The two temperature regions are also clearly seen in Fig. 1 presenting results on

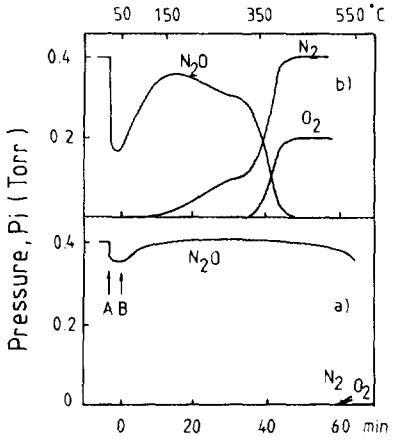

FIG. 1. Temperature-programmed decomposition of N_2O over samples Fe-0.05 (a) and Fe-2.2 (b). The spectra are identical after pretreatment of samples at 550°C both in vacuum and in dioxygen.

temperature-programmed decomposition (TPD) over Fe–Si samples. The experimental procedure was like that in (*15*). After the standard pretreatment at 550°C the samples were cooled to 50°C and N_2O (0.4 Torr) was fed into a reactor volume (1 Torr = 133.3 N/m^2). At the moment "A" the microreactor was opened up and, when the adsorption equilibrium point was reached, the temperature-programmed heating was switched on (moment "B", 8°C/min).

Figure 1a shows the TPD picture for the Fe-0.05 sample. That is typical of samples having no α-sites. Temperature growth leads to complete N_2O desorption and, thus, $P(N_2O)$ regains its initial value which remains constant if the temperature is below that of the start of decomposition via reaction (2). The temperature of such a "high temperature" decomposition depends on the catalytic activity of a sample. In the case of Fe-0.05 which is of quite low activity the remarkable decomposition does not start until 500°C.

An essentially different picture is observed with Fe-2.2 sample. α-Sites are evidenced here to be available. $P(N_2O)$ is seen not to regain its initial value because a "low temperature" decomposition begins at the temperature as low as 120°C prior to the completion of N_2O desorption and results in binding oxygen to a surface and evolution of N_2 (reaction 1). As in case of Fe–Al–Si samples the desorption of O_2 does not start until ca. 300°C (the beginning of the region of "high temperature" catalytic decomposition) and becomes completed at ca. 400°C, stoichiometric amounts of N_2 and O_2 in a gas phase being caused by the decomposition.

A modified experiment with temperature-programmed heating was carried out on Fe-2.2 to examine α-oxygen desorption without N_2O in a gas phase. A distinction between this experiment and the former one is that at 250°C heating was interrupted and, after evacuation of gas phase, started up again. Similarly to the preceding experiment, evolution of O_2 begun at ca. 300°C.

Table 1 presents α-site concentrations ($C_{\alpha-s}$) on the ferrisilicates. Two methods were used to determine $C_{\alpha-s}$ values: (i) measuring N_2 evolved till the completion of reaction (1) at 250°C and (ii) measuring the rate of isotopic homomolecular O_2 exchange (*21*),

$$^{18}O_2 + {}^{16}O_2 \rightarrow 2\,{}^{16}O^{18}O, \qquad (3)$$

which is proportional to the number of α-sites with preloaded α-oxygen atoms. The results of both methods are in good agreement. Owing to catalytic nature of reaction (3) the latter method allows measurement of low α-site concentrations (as low as 1×10^{16} site/g).

The reactivity of α-oxygen on Fe–Si samples is of great interest to study. For this purpose the reactions of CO and CH_4 oxidation along with isotopic O_2 exchange were examined. Their results are not presented here since they are identical to the earlier results obtained with Fe–Al–Si samples (*15*, *16*). α-Oxygen on Fe–Si samples proved also to be of very high reactivity. At room temperature α-oxygen becomes involved in O_2 isotopic exchange as well as in oxidation of CO and CH_4. The stoichiometry of oxidation, as in the case of Fe–Al–Si, corresponds to the interaction of one α-atom with a molecule of CO or CH_4.

It is worth mentioning that the low temperature N_2O decomposition is not caused by the reduction of FeZSM-5 samples during the high temperature pretreatment. Special experiments with Fe-2.2 and other zeolite samples demonstrated that there is no O_2 uptake after vacuum pretreatment (550°C, 2 h) over the temperature range from 50 to 550°C. Completely identical TPD spectra are therefore produced irrespective of the pretreatment procedure (Fig. 1). The inertia of α-sites with respect to O_2 explains the absence of effect of dioxygen on both low and high temperature decomposition of N_2O.

These are the reasons for the essential difference between FeZSM-5 zeolites and metal oxides (MnO_2, CuO, NiO, Cr_2O_3, Fe_2O_3, etc.). Iron oxide, whose properties are the typical ones of the oxides, was stud-

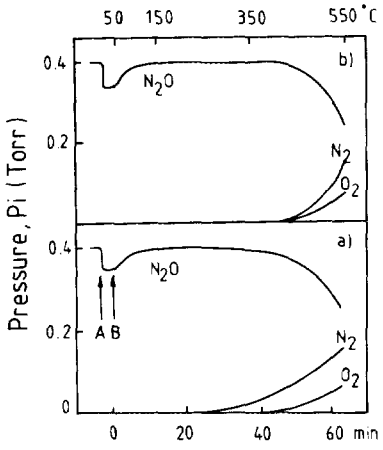

FIG. 2. Temperature-programmed decomposition of N_2O over Fe_2O_3/SiO_2-3.0 after pretreatment at 550°C in vacuum (a) and in dioxygen (b).

ied more thoroughly in both bulk and supported forms (Table 1). Figure 2 presents TPD data for the Fe_2O_3/SiO_2-3.0 sample. Some N_2O decomposition is seen to occur in low temperature region too (300–400°C) after the vacuum pretreatment, oxygen being bound to a surface (Fig. 2a). But this is only a seeming similarity to FeZSM-5 samples having α-sites. Test reactions (isotopic O_2 exchange, CO oxidation) demonstrated no reactivity of this oxygen. Unlike α-oxygen form, it is inert at room temperature. Furthermore, TPD experiments after pretreatment in oxygen (Fig. 2b) showed that the low temperature N_2O decomposition observed in the preceding experiment occurred due to partial reduction of surface during vacuum pretreatment of Fe_2O_3/SiO_2-3.0.

Catalytic properties of Fe-containing samples studied are illustrated in Table 1 where the reaction rate is related to various parameters of a catalyst: W_g to catalyst weight; W_{Fe} to the number of Fe atoms; TOF (turnover frequency) to the number of active α-sites. In the cases of FeZSM-5 and Fe_2O_3/SiO_2-3.0 W_{Fe} referred to the total number of Fe atoms in the sample; in case of bulk Fe_2O_3, to the number of surface Fe atoms (assumed density 10^{19} Fe/m^2).

DISCUSSION

1. Comparison of FeZSM-5 Zeolites (Ferrisilicates to Ferrialuminosilicates)

Figure 3 shows catalytic activity as a function of iron concentration. The curve is plotted with the data of Table 1. The reaction rate W_g is seen to increase by three orders of magnitude as C_{Fe} grows and to trend towards a rate limit. The reaction rates observed with the two samples of minimum iron content (Fe-0.003 and Fe-0.05) are equally low and likely to correspond to the "background" activity (independent of iron) of the zeolite matrix.

The curve of the same dependence for the Fe–Al–Si system (*16*) is also represented in this figure in order to compare it to that of the preceding example. As a whole, the second curve takes after the first one in its shape but is significantly shifted from it with respect to iron content. Thus, the Fe–Si sample should have 10–100 times the iron content of the Fe–Al–Si sample of equal activity. And, vice versa, in some instances equal Fe contents result in different activities of the samples, the activity of Al-containing samples being greater by two orders of magnitude than that of the samples not containing Al. Such a strong effect of aluminium suggests that Al atoms take part, along with Fe, in the formation of active sites. Al is well known as the key element for

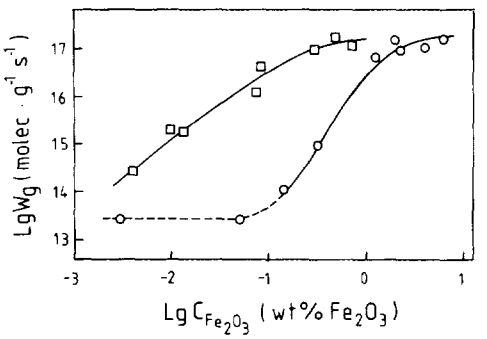

FIG. 3. Dependence of the reaction rate on iron concentration in ZSM-5 zeolites of Fe–Si–O (○) and Fe–Al–Si (□) composition.

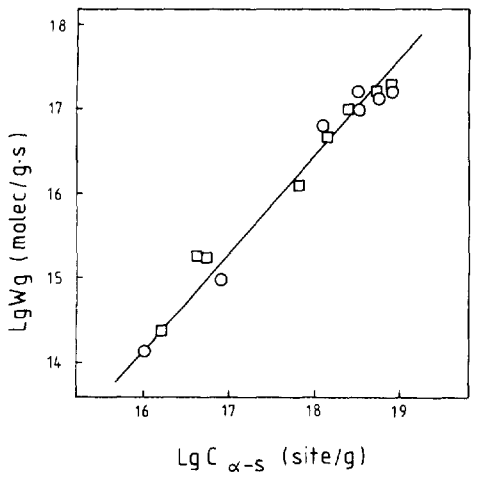

FIG. 4. Dependence of the reaction rate on the active α-sites concentration in ZSM-5 zeolites of Fe–Si (○) and Fe–Al–Si (□) composition.

catalytic properties of zeolites in acid–base reactions.

The chemical composition of active sites in Fe–Si systems can easily be found in a direct way by comparing concentrations of α-sites and Al. As mentioned above, the aluminium admixture in Fe–Si zeolites is 0.01–0.03 wt% Al_2O_3; i.e., it corresponds to (1.2–3.6) $\times$ 10^{18} Al/g. The $C_{\alpha-s}$ of the samples with the highest iron content is seen to be above this value (Table 1), and the assumption of aluminium being incorporated in the active sites is therefore excluded.

As to Fe–Al–Si zeolites, the results of such a comparison cannot be interpreted unambiguously since the aluminium concentration here is about 2 $\times$ 10^{20} atom/g, much higher than the $C_{\alpha-s}$ value. However, the above conclusion may be recognized as valid for both systems due to the identity of the properties of their active sites.

To illustrate this, the rate of N_2O decomposition as a function of α-site concentration is shown in Fig. 4. In contrast to Fig. 3, where the two systems give two curves shifted from each other, one can see that here changes of reaction rates by several orders of magnitude are depicted by a common linear function with 45° slope. It is therefore the number of active α-sites that determines the catalytic properties of the samples, whereas the activity of a site (turnover frequency) remains constant in all the cases.

Not only the equal reaction rates at a certain temperature argue in favour of identity in properties of the active sites, but also the equality of their temperature dependencies does. Figure 5 represents the Arrhenius plots of TOF for Fe–Si and Fe–Al–Si systems. All the data are satisfactorily depicted by a common function corresponding to 28–30 kcal/mol activation energy. In case of different chemical compositions of active sites the coincidence would hardly be probable.

2. *Peculiarities of the Active State of Iron in FeZSM-5*

The above data show catalytic properties of FeZSM-5 zeolites to be determined by specific active sites composed of Fe atoms. These α-sites are inert to O_2 and their peculiarity is the ability to activate N_2O decomposition, thus producing a new reactive form of surface oxygen.

The formation of α-sites causes a substantial change in the state and properties of Fe atoms. Such a conclusion can be based on the data obtained with three types of Fe-containing samples (Table 2): Fe_2O_3, Fe_2O_3/SiO_2-3.0, and Fe-4.0. The second sample has nearly the same iron content as the third one (3.0 and 4.0 wt% Fe_2O_3) but their silicate matrix structures differ from each other; amorphous SiO_2 for the former and ZSM-5 for the latter. The samples were studied not only in N_2O decomposition, but also in the reaction of isotope O_2 heteroexchange, i.e., redistribution of isotopes between oxygen on the surface and dioxygen in a gas phase:

$$^{18}O_2 + {}^{16}O_{surf} \rightarrow {}^{18}O^{16}O + {}^{18}O_{surf}. \quad (4)$$

The rate of this reaction depends on the bond energy of surface oxygen and is treated as characteristic of its reactivity with re-

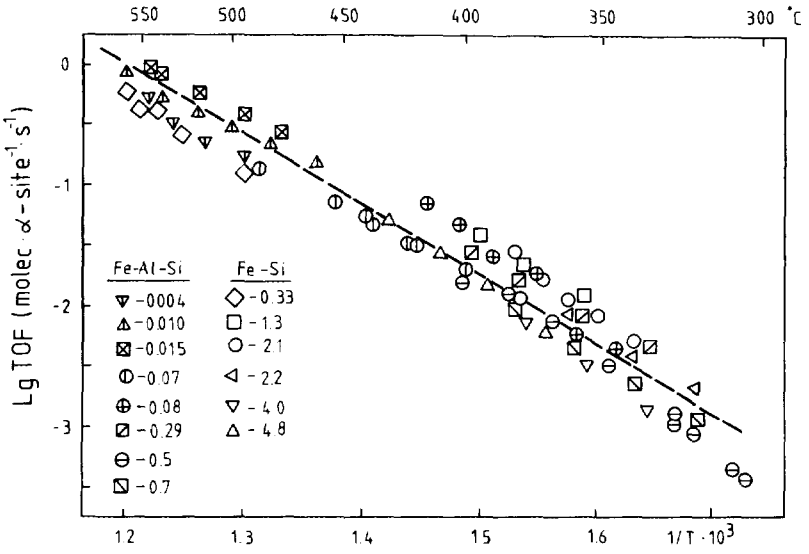

FIG. 5. Arrhenius plot of turnover frequencies (TOF) for ZSM-5 zeolites of Fe–Si (open signs) and Fe–Al–Si (marked signs) composition with different content of iron (wt% Fe_2O_3).

spect to oxidation reactions (*22*). We should recall that isotopic exchange of "intrinsic" surface oxygen is under consideration here but not the exchange of α-oxygen produced by N_2O decomposition. (As to the reactivity of α-oxygen, we have already mentioned that reaction (4) with its participation readily proceeds at room temperature).

Comparison of the data for Fe_2O_3 and Fe_2O_3/SiO_2-3.0 indicates no significant changes in the properties of Fe with respect to either N_2O decomposition or oxygen exchange. Comparatively slight differences in atomic reaction rates W_{Fe} may be attributed to an uncertainty in the dispersity of the supported oxide.

Comparison of Fe_2O_3 with Fe-4.0 evidences that introduction of Fe in a zeolite matrix gives rise to more substantial changes in the state of Fe. The nature of the changes is of the kind which produces an opposite effect on the reactions. Thus, in the reaction of N_2O decomposition the atomic rate $W_{Fe}(N_2O)$ increases by two or-

TABLE 2

Catalytic Properties of Fe in Some Fe-Containing Samples

Sample	N_2O decomposition			Isotopic O_2 exchange		
	Δt (°C)	E_{act} (kcal · mol^{-1})	W_{Fe}[a] (molecule · Fe^{-1} · s^{-1})	Δt (°C)	E_{act} (kcal · mol^{-1})	W_{Fe}[b] (molecule Fe^{-1} · s^{-1})
α-Fe_2O_3	470–550	33 ± 1.5	$4.0 \cdot 10^{-6}$	345–450	28	$1.3 \cdot 10^{-4}$
Fe_2O_3/SiO_2-3.0	480–550	32 ± 3	$1.0 \cdot 10^{-6}$	400	—	$6.0 \cdot 10^{-5}$
Fe-4.0	340–400	31 ± 3	$2.7 \cdot 10^{-4}$	475–545	52	$2.5 \cdot 10^{-8}$

[a] At 400°C, $P(N_2O) = 0.4$ Torr.
[b] At 400°C, $P(O_2) = 0.4$ Torr.

ders of magnitude due to the high concentration of α-sites formed (3.5×10^{18} site/g, Table 1). In contrast to that, a dramatic decrease in catalytic activity occurs in the reaction of isotopic oxygen exchange due to the loss of ability to activate O_2. This causes a decrease of the atomic rate $W_{Fe}(O_2)$ by four orders of magnitude and an increase in the activation energy from 28 to 52 kcal/mol.

These results cannot be explained by dispersal of the Fe_2O_3 phase, they argue in favour of more profound changes in the state of Fe. The state of Fe incorporated in α-sites is of considerable interest. Our attempts to employ a number of techniques (NMR, IR, UV-VIS, EXAFS, ESR) failed to give reliable information. The task is complicated by the fact that when a high fraction of Fe atoms involved in the active state (e.g., in some samples of Fe–Al–Si samples $C_{\alpha-s}/C_{Fe}$ = 20–25% (*15*)), the total content of iron proved not to be sufficient for reliable measurements. On the contrary, for the samples with high iron content the fraction of active Fe atoms proves to be too low (1–2% for the Fe–Si system, Table 1) to be distinguished from other states.

ESR is one of the most sensitive and widely used methods to study the state of iron in zeolites (*23–27*). We have taken ESR spectra of nearly all the FeZSM-5 samples of both Fe–Si and Fe–Al–Si composition (ESR-221 spectrometer, room temperature in air). In accordance with the literature, there are two main signals in the spectra of these samples with g-values 4.3 and $\approx$2. The signal with g = 4.3 is usually assigned to Fe^{3+} ions, which substitute for Si^{4+} in the tetrahedral position of the lattice framework. The broad signal with $g \approx 2$ is assigned to Fe^{3+} in nonlattice positions. We have tried to connect the catalytic activity of Fe–Si and Fe–Al–Si zeolites with either of these cases of iron but no correlation has been found. One of the possible reasons may be that the active state of iron responsible for N_2O decomposition is invisible for ESR. This assumption is consistent with the quantum chemical model of active sites formulated in (*28*) to interpret our data.

According to the model, the active α-sites are the minimum cluster $[Fe_2O_3 \cdot 2H_2O]$ of oxide-like phase whose formation occurs as iron escapes from the ZSM-5 lattice during thermal treatment of samples. The calculated energy for oxygen atom interaction with the cluster to produce the complex $[O \cdot Fe_2O_3 \cdot H_2O]$ is confirmed by calorimetric measurements of α-oxygen formation from N_2O decomposition (*29*). An oxygen atom of the complex $[O \cdot Fe_2O_3 \cdot H_2O]$ should readily participate in oxidation reactions since energy consumption for cleaving the Fe–O bond should be mainly compensated owing to strengthening other bonds in the complex.

As to the influence of aluminium, it is presumably connected with its role in the mechanism of α-site formation. The presence of Al should facilitate the removal of Fe from a zeolite lattice thus providing a higher concentration of the active sites at the same iron content.

In conclusion we would like to notice that though the model discussed can explain some important features of FeZSM-5 zeolites, many issues still remain unclear. For instance, what is the nature of the uniqueness of iron and why other metals are not active? Is this the consequence of their inability to form proper complexes or inability of the complexes to active N_2O? How important is the structure of ZSM-5 zeolite and is it possible for α-sites to exist in zeolite matrices of other types?

All these and other questions initiate further experimental and theoretical study.

REFERENCES

1. Golodets, G. I., "Heterogeneous Catalytic Reactions Involving Molecular Oxygen." Elsevier, Amsterdam, 1983.
2. Shepelev, S. S., and Ione, K. G., *React. Kinet. Catal. Lett.* **23,** 319 (1983).
3. Liu, H. F., Liu, R. S., Liew, K. Y., Johnson, R. E., and Lunsford, J. N., *J. Am. Chem. Soc.* **106,** 4117 (1984).
4. Zhen, K. J., Khan, M. M., Mac, C. H., Lewis, K. B., and Somorjai, G. A., *J. Catal.* **94,** 501 (1985).

5. Anderson, J. R., and Tsai, P., *J. Chem. Soc., Chem. Commun.* 1435 (1987).
6. Il'chenko, N. I., Bostan, A. I., Dolgikh, L. Y., and Golodets, G. I., *Teor. Eksp. Khim.* **23,** 641 (1987).
7. Vereshchagin, S. N., Shishkina, N. N., and Anshits, A. G., "New Developments in Selective Oxidation." (G. Genti and F. Trifiro, Eds.). Bologna, 1989.
8. Hutchings, G. J., Scurell, M. S., and Woodhouse, J. R., *Chem. Soc. Rev.* **18,** 251 (1989).
9. Iwamoto, M., Hirata, J., Matsukami, K., and Kagawa, Sh., *J. Phys. Chem.*, **87,** 903 (1983).
10. Suzuki, E., Nakashiro, K., and Ono, Y., *Chem. Lett.* 953 (1988).
11. Gubelmann, M., and Tirel, Ph., French Patent 2630735 (filed May 2, 1988).
12. Kharitonov, A. S., Aleksandrova, T. N., Vostrokova, L. A., Ione, K. G., and Panov, G. I., Soviet Authorship Certificate 4445646 (filed June 22, 1988).
13. Gubelmann, M., and Tirel, Ph., U.S. Patent 5001280 (1991).
14. Kharitonov, A. S., Romannikov, V. N., Sheveleva, G. A., Sobolev, V. I., Panov, G. I., and Ione, K. G., Soviet Authorship Certificate 4746635 (1991).
15. Panov, G. I., Sobolev, V. I., and Kharitonov, A. S., *J. Mol. Catal.* **61,** 85 (1990).
16. Panov, G. I., Sobolev, V. I., and Kharitonov, A. S., *in* "Catalytic Science and Technology" (S. Yoshida, N. Takezawa, T. Ono, Eds.), Vol. 1, p. 171. Kodansha, Tokyo, 1991.
17. Panov, G. I., Sheveleva, G. A., Kharitonov, A. S., Romannikov, V. N., and Vostrikova, L. A., *Appl. Catal.* **82,** 31 (1992).
18. Kharitonov, A. S., Sheveleva, G. A., Panov, G. I., Paukshtis, Ye. A., Romannikov, V. N., and Razdobarova, N. L., submitted for publication.
19. Marosi, L., Stabenow, J., and Schwarzman, M., Patent DE 2831611 (1980).
20. Sobolev, V. I., Kharitonov, A. S., and Panov, G. I., *React. Kinet. Catal. Lett.* **29,** 433 (1985).
21. Sobolev, V. I., Ph.D. Thesis. Institute of Catalysis, Novosibirsk, Russia, 1991.
22. Boreskov, G. K., *in* "Catalysis—Science and Technology" (J. R. Andersopn and M. Boudart, Eds.), Vol. 3, p. 39. Springer-Verlag, Berlin/New York, 1982.
23. Iton, L. E., Beal, R. B., and Hodul, T. D., *J. Mol. Catal.* **21,** 151 (1983).
24. Ball, W. J., Dwyer, J., Garforth, A. A., and Smith, W. J., *in* "Proceedings, 7th International Zeolite Conference," p. 137, 1986.
25. Kucherov, A. V., Slinkin, A. A., *Kinet. Katal.* **28,** 1199 (1987).
26. Lin, D. H., Condurier, G., and Vedrine, J. C., *in* "Zeolites: Facts, Figures, Future" (P. A. Jacobs and R. A. Santen, Eds.), p. 1431. Elsevier, Amsterdam, 1989.
27. Ratnasamy, P., and Kumar, R., *Catal. Today* **9,** 328 (1991).
28. Filatov, M. Y., Pelmenshchikov, A. G., Zhidomirov, G. M., submitted for publication.
29. Sobolev, V. I., Kovalenko, O. N., Kharitonov, A. S., Pankratiev, Yu. D., and Panov, G. I., *Mendeleev's Commun.* **1,** 29 (1991).